Cement & Concrete Composites 34 (2012) 1104–1113

Contents lists available at SciVerse ScienceDirect

Cement & Concrete Composites

journal homepage: www.elsevier.com/locate/cemconcomp

Dispersion of carbon nanotubes and its influence on the mechanical properties of the cement matrix

Anastasia Sobolkina [a], Viktor Mechtcherine [a,*], Vyacheslav Khavrus [b], Diana Maier [b], Mandy Mende [c], Manfred Ritschel [b], Albrecht Leonhardt [b]

[a] Institute of Construction Materials, Faculty of Civil Engineering, Technische Universität Dresden, D-01062 Dresden, Germany
[b] Leibniz Institute for Solid State and Materials Research (IFW), Dresden Helmholtzstrasse 20, D-01069 Dresden, Germany
[c] Institute of Physical Chemistry and Polymer Physics, Leibniz Institute of Polymer Research Dresden, Hohe Strasse 6, D-01069 Dresden, Germany

ARTICLE INFO

Article history:
Received 2 April 2012
Received in revised form 29 July 2012
Accepted 30 July 2012
Available online 8 August 2012

Keywords:
Carbon nanotubes
Dispersion
Surfactant
Sonication
Cement-based composites
Mechanical properties

ABSTRACT

An appropriate dispersion of carbon nanotubes (CNTs) is a prerequisite for their use in improving the mechanical properties of cement-based composites. In this study two types of carbon nanotubes (CNTs) having different morphologies were investigated. To obtain a uniform distribution of CNTs in the cement matrix, the effect of sonication on the deagglomeration of CNTs in combination with anionic and nonionic surfactants in varying concentrations was quantitatively investigated when preparing aqueous dispersions of CNTs for the subsequent use in cement paste. The relationships between the quality of CNT-dispersion on the one hand and the sonication time and surfactant concentration on the other were determined using UV–vis spectroscopy. After dispersion, nitrogen-doped CNTs were found mostly as individual, broken CNTs. In contrast, after the treatment of the mixture of single-, double-, and multi-walled CNTs, a net-like distribution was observed where destruction of the CNTs due to sonication could not be distinguished. Modification of the cement pastes with dispersions of CNTs led to a pronounced increase, up to 40%, in compressive strength and, in some cases, to a moderate increase in tensile strength under high strain-rate loading. However, no significant improvement in strength was observed for quasi-static loading. Microscopic examination revealed that the bridging of the C–S–H phases differed depending on the type of CNT. This explained, at least partly, the observed effects of CNT-addition on the mechanical properties of hardened cement pastes.

1. Introduction

Carbon nanotubes (CNTs) possess unusually high strength and stiffness and are chemically stable and electrically conductive as well. These properties make the use of CNTs attractive in the design of composite materials based on different matrices [1–6]. Since the first report on CNTs by Iijima in 1991, numerous attempts have been made to strengthen materials (especially polymer-based materials) with nanotubes [7–9]. In the last few years, the effect of CNT-additions to cement-based materials has also been investigated. However, some of the findings reported in the literature are contradictory.

According to Konsta-Gdoutous et al. [10], the addition of short, multi-walled CNTs (MWCNTs) (l/d = 700) in a concentration of 0.08% led to a 35% increase in flexural strength and Young's modulus of the cement paste matrix. Using long MWCNTs (l/d = 1600), a similar improvement of the mechanical properties could be achieved with an even lower CNT content. According to Li et al. [11], the use of chemically functionalized CNTs in a concentration of 0.5% by weight of cement led to an increase in compressive and flexural strength of the mortar of 19% and 25%, respectively. Makar et al. [12] observed an acceleration in cement hydration as a result of a CNT addition (2% by mass of cement) at a young age. However, after longer hydration, almost no differences between the mechanical parameters of the reference samples and the samples modified with CNTs were observed. According to Musso et al. [13], the modification of mortar with functionalised CNTs (0.5% by mass of cement) caused a reduction of approximately 80% in the compressive strength and a reduction of approximately 60% in the modulus-of-rupture.

The widely-differing effects of CNT additions on the mechanical performance of cement materials can likely be explained by the different choices of type and quantity of CNTs and in the methods of dispersing the nanotubes. The published data is insufficient to come to a satisfactory conclusion on this topic.

It has been emphasized repeatedly in the literature [14–16] that CNTs tend towards agglomeration, which impedes their uniform

* Corresponding author.
E-mail address: mechtcherine@tu-dresden.de (V. Mechtcherine).

0958-9465/$ - see front matter © 2012 Elsevier Ltd. All rights reserved.
http://dx.doi.org/10.1016/j.cemconcomp.2012.07.008

distribution within a matrix. Non-uniformly distributed CNTs cannot form a fine, continuous network within a matrix to support load transfer or mitigate the development of cracks. Furthermore, the CNT agglomerates could function as local defects due to their low strength in the direction normal to the tubes' axes. Sàez de Ibarra et al. [17] demonstrated that with the use of the emulgator gum arabic, the deagglomerated CNTs exerted a more positive influence on the mechanical properties of cement paste. Konsta-Gdoutos et al. [14] achieved the best results in terms of strength for the cement paste doped by CNTs which were dispersed in water using sonication and surfactant-to-CNTs weight ratio of 4. Furthermore, the quality of dispersion was estimated by testing rheological behaviour of fresh cement paste and by electron microscopy. Luo et al. [15] showed that the quality of the dispersion of CNTs in water and subsequently the effect of CNTs on mechanical properties depends on the type of surfactant. However, the authors failed to investigate and discuss possible effects of the surfactants as such, i.e., without the addition of CNTs.

There are still many open questions, such as: (a) how to test the compatibility of particular CNTs and surfactants, (b) how the duration and intensity of sonication affect the dispersion of CNTs, and (c) how to avoid the rupture of CNTs during sonication. There are no systematic investigations of this issue yet. Furthermore, there is little knowledge of the shape and length of CNTs in the hardened cement paste, as well as what is their position relative to voids and hydration products. Finally, it is still to be clarified to which extent the strength and stiffness of CNTs have a direct effect on improvement of mechanical properties of hardened cement paste and what are other effects like, e.g. triggering of the formation of high-density C–S–H phases in presence of CNTs.

The purpose of this paper is to clarify some of the above-mentioned open questions. In particular, the effects of sonication and two different surfactants are investigated with respect to the dispersion of two different CNTs in water. Another focus is on characterising the degree of dispersion and the condition of the CNTs in water. Furthermore, the influence of the addition of dispersions with different types of CNTs on the mechanical properties of cement paste under static and dynamic tensile and compression loading is studied. Additional information is provided by morphological investigations of the cement paste, which, in addition to the other results, form the basis for discussion.

2. Materials and methods

2.1. Materials

For this study, two types of CNTs were chosen, whose lengths differed by one order of magnitude.

The first type was a mixture of single-, double-, and multi-walled CNTs (hereinafter "mixed CNTs"). The fixed-bed chemical vapour deposition (CVD) method utilized for synthesis of the mixed CNTs led to their agglomeration in bundles; cf. Fig. 1a and b. The ratio of single- and double-walled CNTs to multi-walled CNTs was approximately 1:1. The mixed CNTs measured approximately 20 μm in length at a diameter of approximately 1–15 nm. Fig. 1b shows that the single-wall CNTs form intertwining strands with a diameter of up to approximately 20 nm, resulting from the agglomeration. The mixed CNTs have a typical tubular structure [18]; cf. Fig. 1c.

As the second type, aligned, nitrogen-doped, multi-walled CNTs (hereinafter: N-CNTs) were used. As a result of their synthesis via an aerosol-assisted CVD method, blocks of aligned CNTs were formed; cf. Fig. 1d and e. The length typically measured 100–300 μm at a diameter of approximately 15–40 nm. The application of acetonitrile as a feedstock caused the incorporation of nitrogen into the shells of the CNTs. This led to the formation of internal partition walls within the central core and consequently a bamboo-like structure [18]; cf. Fig. 1f.

In order to remove the solid catalyst material (MgO and free metal catalysts), the mixed CNTs were sonicated for 30 min in hydrochloric acid diluted with distilled water at a ratio of 1:1. After 20 min the CNTs were filtered with a vacuum filtration system and rinsed with distilled water until they reached a pH-neutral value of 7. As the catalyst was fully covered by carbon (in the case of aerosol-CVD), the N-CNTs could be used without chemical treatment (no MgO-support was used). However, they were pre-treated in the same way as the mixed CNTs to ensure the same surface properties.

Because of their strongly hydrophobic surface, CNTs are difficult to disperse in water. In order to reduce the surface tension and to improve the wetting of the CNTs, two different surfactants known from earlier studies [19–21] were used: an anionic sodium dodecyl sulfate (SDS, MW = 288.38 g/mol) and a nonionic polyoxyethylene(23) laurylether (denoted below as Brij 35, MW = 1198 g/mol). One of the selection criteria for the surfactants was, in addition to their good dispersive capacity, their complete dissolution in water at room temperature.

2.2. Preparation of CNT dispersions

Aqueous dispersions were produced with 0.5 wt.% of CNTs related to distilled water. The choice of surfactant contents was based on the optimal CNT-to-surfactant mass ratios given in the literature. For the system CNTs/SDS they were 1:1.5 [22], 1:2 [23], 1:4 [19], 1:520 [24]. Brij 35 reached sorption maximum on the CNT surface at a concentration of approximately 100 mg L^{-1}, while the amount of CNTs in the solution measured 100 mg L^{-1} [21]. For this study the following CNT-surfactant ratios for dispersion of CNTs were initially chosen: 1:0, 1:1, 1:2. The minimum CNT-to-surfactant ratio for N-CNTs was set at 1:0.24 for SDS and 1:0.02 for Brij 35. In the Results section, the surfactant contents are converted into molarity.

The dispersion of the CNTs in water containing surfactant was accomplished using sonication by means of a cup-horn high intensity ultrasonic homogenizer (SONOPULS) with a cylindrical tip. The sonicator was operated at an amplitude of 70% of the maximum (one of which was 210 micrometer). The durations of sonication were 30, 150, and 210 min. Sonication lasting less than 30 min was unsatisfactory with regard to the quality of the dispersions (since the large agglomerates of CNTs scattered light, no clear absorption peak on the UV–vis spectra was observed; cf. Section 2.3) and was accordingly not considered further. To avoid evaporation of the water during sonication, the glass container was covered and cooled.

2.3. Characterisation of the degree of dispersion of CNTs

The extent of CNT-dispersion in water relative to the variation of the duration of sonication and surfactant concentration was evaluated using ultraviolet–visible spectroscopy (UV–vis spectroscopy). In the UV–vis measurements, the CNTs display the characteristic peaks in the ultraviolet spectral region [22,23] (in this case, at a wavelength of 260 nm for both kinds of CNTs). According to the Beer–Lambert Law, the absorbance of a solution A is directly proportional to its molar concentration c at a constant layer thickness d and subject as well to the material-specific constant ε, the molar extensity coefficient [in cm^2/mmol] (Eq. 1):

$$A = -\log(I/I_0) = \varepsilon \cdot c \cdot d, \quad (1)$$

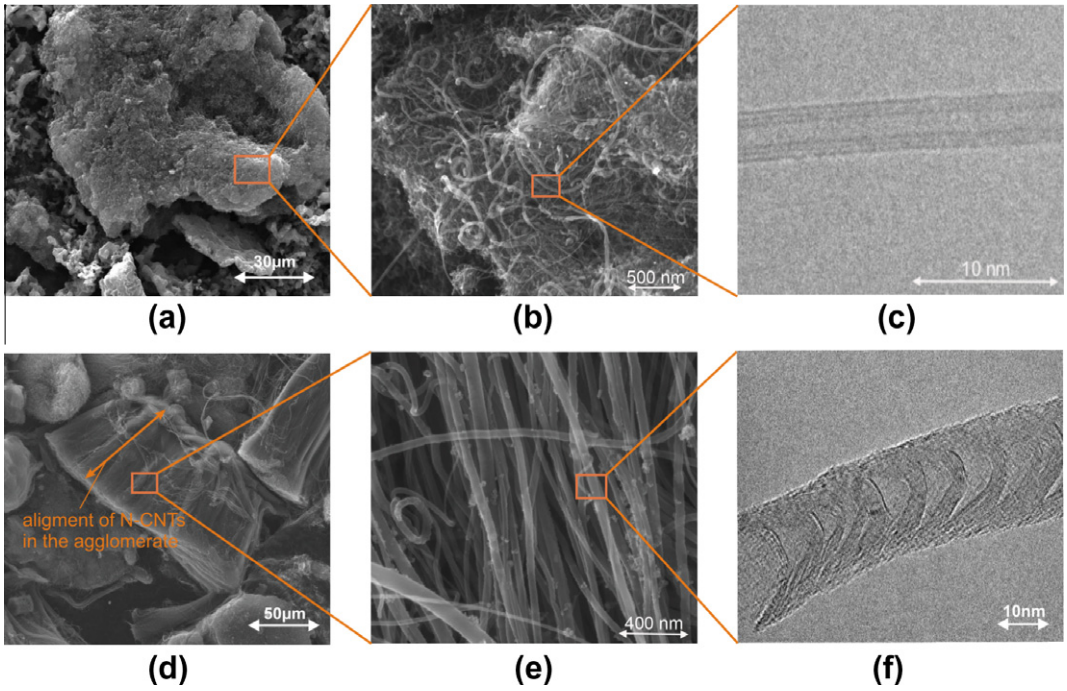

Fig. 1. Scanning electron microscope images of agglomerates of (a and b) mixed CNTs and (d and e) N-CNTs; transmission electron microscope images of (c) the tubular structure of mixed CNTs and (f) the bamboo-like structure of N-CNTs.

where I_o und I are the intensity of the incident light and the transmitted light, respectively,

Fig. 2 clearly shows that absorbance increases with increasing sonication time, which can be traced back to the dissaglomeration of CNTs and their finer dispersion in water. Accordingly, the absorbance value was used to quantify the degree of dispersion of the CNTs.

The solutions were prepared by diluting the sonicated dispersions with distilled water in a ratio of 1:300 shortly before taking measurement. Since overlappings of the bands of surfactant and CNT were possible in the UV–vis measurements, the spectra of surfactant solutions were measured and baseline corrections performed.

A relationship among the influence factors (i.e., surfactant concentration x_1 and sonication time x_2), and the absorbance of aqueous CNT dispersions y was established with the help of the approximation method, namely the design of experiment (DOE) [25–27]. In order to describe the correlation among the variables and so replicate a linear model, the following regression was used:

$$y_i = b_0 + b_1x_{1i} + b_2x_{2i} + b_3x_{1i}^2 + b_4x_{1i}x_{2i} + b_5x_{2i}^2 + b_6x_{1i}^2x_{2i} + b_7x_{1i}x_{2i}^2, \quad (2)$$

where b_0 – regression constant; b_1, $b_2 \ldots b_7$ – regression coefficients; $i = 1, 2 \ldots n$, n – number of tests. The agreement between the model functions and the real measurement data was verified with the F-test. The obtained Fischer criteria did not exceed the critical value of 18.5, which corresponded to the 5% level of significance. Interpolating, the DOE made possible the estimation of values for various combinations of the influence factors for which measurements were not performed. It should be underlined that the DOE method was used here for the clear display of the tendencies only. No generalised predictions of the effect of individual parameters were envisaged.

The condition of the CNTs after sonication was studied by examinations of dispersion films using scanning electron microscopy (SEM, here: FEI NOVA NANOSEM-200 at an acceleration voltage of 15 kV). The surfactant adsorption layer on the CNT surface was examined by means of transmission electron microscopy (TEM, here: FEI Tecnai T20, an acceleration voltage of 200 kV was used).

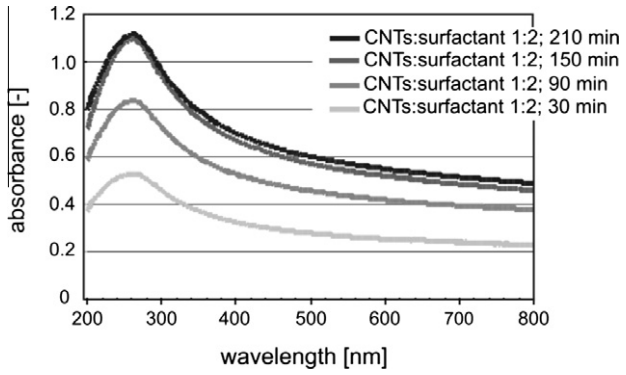

Fig. 2. UV–vis spectrum of aqueous dispersions of the CNTs subject to sonication time; SDS was used as surfactant.

2.4. Production and testing of the CNT-modified cement paste samples

The mixtures were produced using a basis of Portland cement CEM I 42.5 R. The CNT contents (solid matter) were set at 0.05% and 0.25% by cement weight. The CNTs were added to the cement as dispersions within the mixing water. On the basis of the CNT-dispersion results established by UV–vis spectroscopy, DOE, CNT-to-surfactant ratio of 1:1, and a sonication time of 120 min were used to prepare all dispersions used with cement paste. The amount of water contained in the dispersion was considered in the water-to-cement value, which was 0.50 for all mixtures. To observe the influence of surfactants on the properties of cement paste, additional reference samples with a surfactant concentration of 0.25% by weight of cement were prepared. Because the use of Brij 35 and especially SDS was accompanied by the

substantial production of foam, a foam-reducing agent was added, measuring half of the surfactant mass.

After mixing, dumbbell-shaped cylinders with diameters of 2 and 4 mm were produced for compression and tension tests, respectively (Fig. 3a). The forms were filled with cement paste using a syringe and were compacted within 1 min using a vibrating table. After demoulding at an age of one day, the specimens were stored for 27 days in water. Subsequently, uniaxial quasi-static (strain rate $2 \times 10^{-5}\,s^{-1}$) and dynamic ($50\,s^{-1}$) compression and tensile tests were performed with the equipment based on piezoactuators (Fig. 3b). The choice of dynamic testing regime additional to the quasi-static one should provide information of possible different effects of CNTs on the mechanical performance of hardened cement paste at different strain rates. At least ten specimens were tested for every parameter combination.

The hydration of the cement was stopped after 3 and 28 days with isopropanol. The structure of the cement paste was examined with the SEM with the NANOSEM from FEI using a Helix detector, which enabled the study of hydrated cement samples without drying and altering their microstructures by coating them. The porosity of the hardened cement paste was determined using mercury intrusion porosimetry.

3. Results and discussion

3.1. Investigation of the properties of the aqueous CNT-dispersion

Fig. 4 shows the absorbance measured for the dispersions of mixed CNTs and its relationships to the molar concentrations of the surfactants and sonication time as determined by the DOE. The data yield few differences between the dispersions containing SDS and Brij 35. The diagrammes can be divided into three areas. In Area I, the extension of sonication time from 30 to 210 min had almost no influence on the absorbance of dispersions which contained little surfactant in molar concentrations of up to approximately 6 mM of SDS (Fig. 4a) and 1.5 mM for Brij 35 (Fig. 4b). An increase in the concentration of the surfactants was accompanied by a rise in absorbance. In Area II, i. e., molar concentrations of up to approximately 20 mM for SDS and 5 mM for Brij 35, the absorbance (and therefore deagglomeration of CNTs) clearly increased, from approximately 0.4–1.1, with increasing sonication time. However, for sonication times beyond 120 min, no further improvement worth considering could be observed. An increase in the concentration of surfactants also led to an increase in absorbance. In Area III, a further increase in surfactant concentration did not lead to an increased amount of absorbance by the samples; however, the effect of the increasing sonication time on absorbance remained pronounced.

The behaviour described can be explained by the theory of micelle formation [28]. Fig. 5 shows the schematic arrangement of the adsorbed molecules of a surfactant on the CNT surface with increasing concentrations of surfactant. The hydrophilic head groups are pointed outwards and the remainder of the hydrocarbon inwards. In the case of low surfactant concentrations, the quantity of surfactant is not sufficient to coat the surface of the CNTs evenly; cf. Fig. 5-I, which leads to strong surface effects between the CNTs. This complicates the dispersion and allows CNT-agglomerations to persist. After reaching a critical concentration, the surface of the CNT is completely covered with surfactant molecules, which in turn stops the interactions between individual CNTs; cf. Fig. 5-II. The rod-like micelles formed in this process are impeded from forming new agglomerates by their mutual electrostatic repulsion or steric hindrance. A further increase in surfactant content leads to the formation of multilayers of surfactant molecules on the surface of the CNT, which does not improve the CNTs' dispersion in water and can even lead to CNT-flocculation [24].

The critical concentration which scarcely leads to any further improvements in the deagglomeration of the mixed CNTs amounted to approximately 20 mM for SDS and 5 mM for Brij 35, which significantly exceeded the critical concentration of micelle formation (CMC) (8.1 mM for SDS; 0.06…0.1 mM for Brij 35) described in the literature [29,30]. This can be explained by the increase in specific CNT surfaces during dispersion, and for very thin CNTs with large length-to-diameter ratios more surfactant molecules must be available for complete saturation than would be necessary for the aggregation of a ball-like micelle in water. According to [31], in a binary system surfactant micelles tend to dissociate, preferring to associate with the solid phase. The degree of saturation was reached on the CNT surface with SDS molecules at a molar concentration approximately four times higher than was the case with Brij 35. This is due to the small size of the SDS molecules in comparison to Brij 35. For this reason a large number of molecules are necessary to cover the surface completely.

Fig. 6 shows the changes in absorbance of the N-CNT dispersions. The diagrammes can likewise be distinguished by the three areas of change in absorbance already described. The N-CNTs show higher absorbance in the dispersions with Brij 35 than in the dispersions with SDS. For example, at the CNT-to-surfactant ration of 1:1, samples containing Brij 35 have the same absorbance after 30 min of sonication reached by samples containing SDS only after 150 min. This may be traced back to the better deagglomeration of the N-CNTs using Brij 35, in turn due to the better affinity of Brij 35 molecules and N-CNT surfaces. To investigate this assumption more closely, the surfaces of N-CNTs in dispersions were characterised using transmission electron microscopy.

Fig. 7 shows the TEM images of the N-CNTs in dispersions with both surfactants in varying concentrations. The images show that a rise in surfactant content increases the adsorption layer on the surface of the CNT. For low surfactant concentrations (0.1 mM for Brij 35 and 4.2 mM for SDS; cf. Fig. 7a and d), only local areas where the thickness of the adsorbed surfactant reaches several nanometers

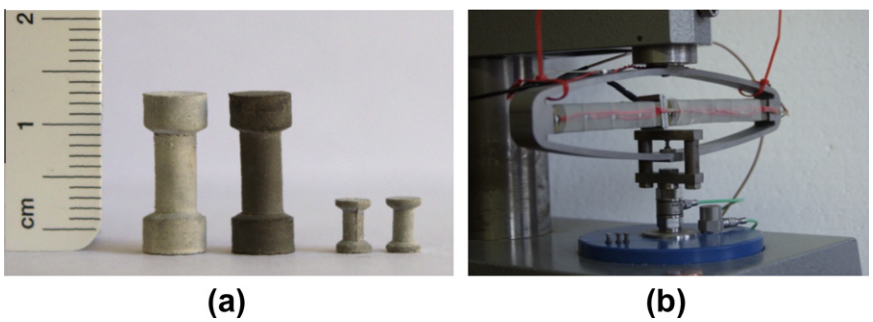

Fig. 3. (a) Samples for tensile test (*left*) and compression test (*right*). (b) Arrangement of samples in the equipment based on piezoactuators.

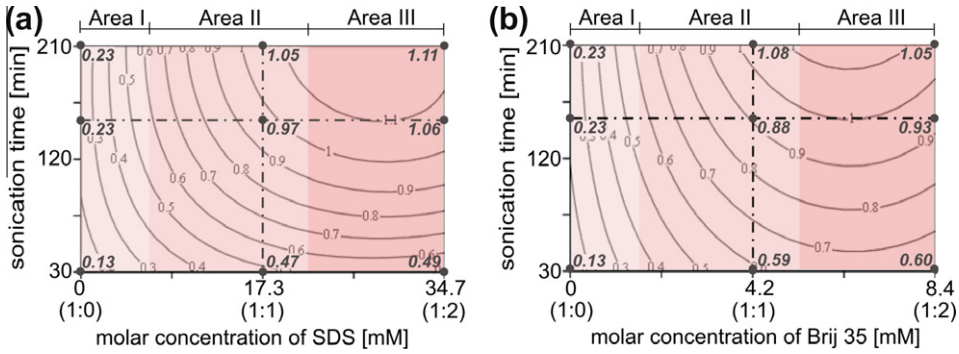

Fig. 4. Change of absorbance in the dispersions of mixed CNTs in dependency on variation of surfactant concentration and sonication time: the cursive numbers are the experimentally obtained absorbance values; the respective CNT-to-surfactant weight ratios are given in parentheses.

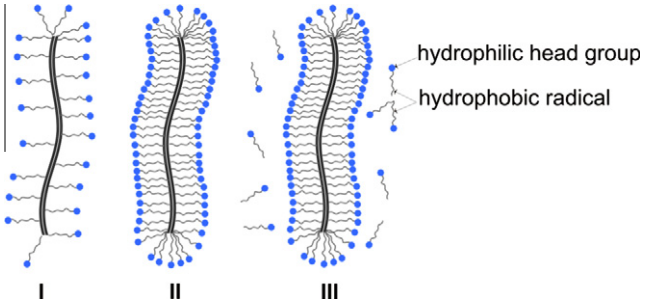

Fig. 5. Schematic representation of the arrangement of adsorbed surfactant molecules on the CNT surface: I – low surfactant concentration, formation of adsorption layers on the CNT surface; II – condition of equilibrium, adsorption layer saturated with surfactant molecules, i.e. formation of rod-like micelles; III – oversaturated surfactant concentration, formation of multiple layers of surfactant molecules on the CNT surface.

can be distinguished. Increasing the Brij 35-content to 4.2 mM (Fig. 7b) leads to complete coverage of the N-CNTs and the formation of an adsorption layer measuring 5–10 nm. In contrast, a selective adsorption is evident in the case of SDS. At a molar concentration of 17.3 mM (Fig. 7e), an uncovered surface of the N-CNTs is present next to the areas with an adsorption layer measuring over 10 nm. SDS molecules gather between the N-CNTs instead of associating with the solid phase. A further increase in surfactant content up to a CNT-to-surfactant ratio of 1:2 leads to the formation of multiple Brij 35 adsorption layers on the interface; cf. Fig. 7c. No direct, even adsorption was observed with high concentrations of SDS; cf. Fig. 7f.

The poor affinity between SDS and N-CNTs can likely be explained by their mutual electrostatic repulsion. According to [32,33] nitrogen atoms incorporated in the graphite lattice of N-CNTs indicate an enhanced reductive effect, which is due to the free electron pairs of the pyridic groups in neutral or alkaline environments. Negativity of the N-CNT surface associated with this effect might cause electrostatic repulsion of SDS molecules.

To determine the state of CNTs after sonication, the dispersion films put on the sample holder and dried were examined using scanning electron microscopy (SEM). In comparison to initial observations SEM images show an obvious reduction in length of the N-CNTs due to sonication; cf. Fig. 8a and b. After 30 min of sonication, the large share of the agglomerations was still identifiable where N-CNTs remained relatively long. In addition, individual short N-CNTs with lengths up to several micrometers were found. The portion of these short N-CNTs grew as the duration of sonication increased. Thus, ultrasonication at the amplitude of 147 μm used leads not only to a disentanglement of the N-CNT agglomerates, but also to ruptures in the CNTs. This can likely be traced back to the low flexibility and high brittleness of N-CNTs due to their relatively large diameters and the presence of internal partition walls [34–36].

During the dispersion of the mixed CNTs, a finely distributed CNT network was formed (Fig. 8c and d), whose density increased during extended sonication. Due to their intertwining and their formation of nets, the destruction of these CNTs by strong cavitation could not be observed.

3.2. Investigation of the CNT-modified, hardened cement paste

In the next step the influence of CNTs on the mechanical properties of hardened cement paste was investigated. Fig. 9a and c shows the results for quasi-static loading. The application of SDS as a surfactant led to a severe drop in the strength of the hardened

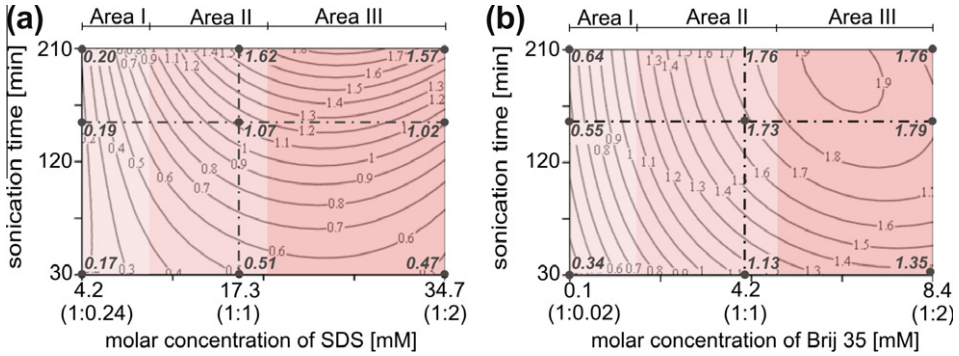

Fig. 6. Change of absorbance in the dispersions of N-CNTs in dependency on variation of surfactant concentration and sonication time: the cursive numbers are the experimentally obtained absorption values; the respective CNT-to-surfactant weight ratios are given in parentheses.

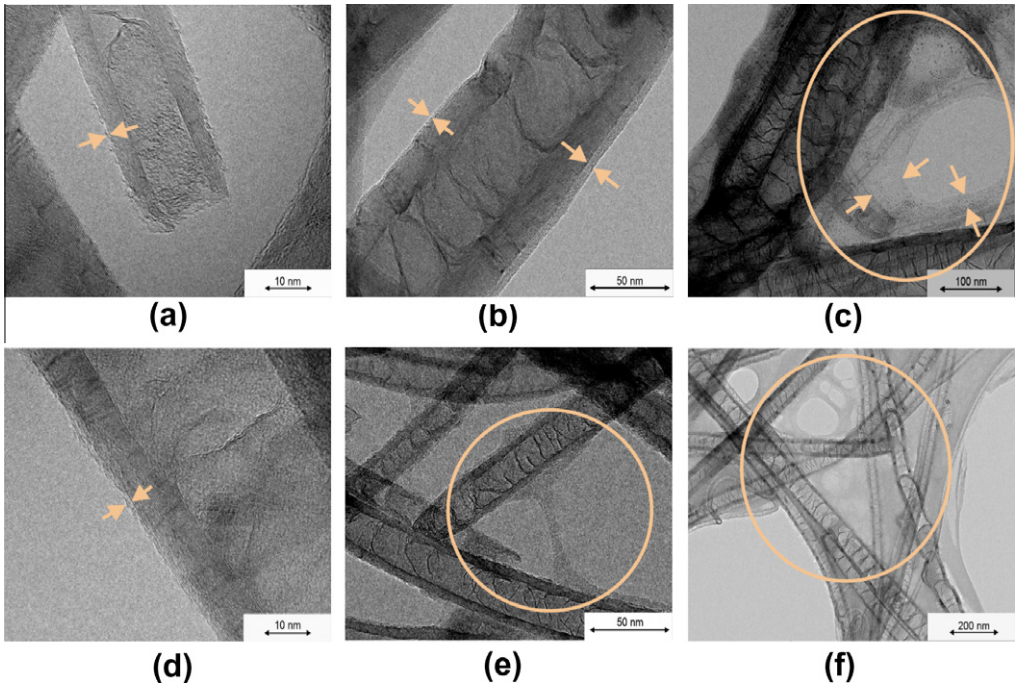

Fig. 7. TEM images of N-CNTs in dispersions after 150 min of sonication using Brij 35 in concentrations of (a) 0.1 mM, (b) 4.2 mM, (c) 8.4 mM; using SDS in concentrations of (d) 4.2 mM; (e) 17.3 mM and (f) 34.7 mM.

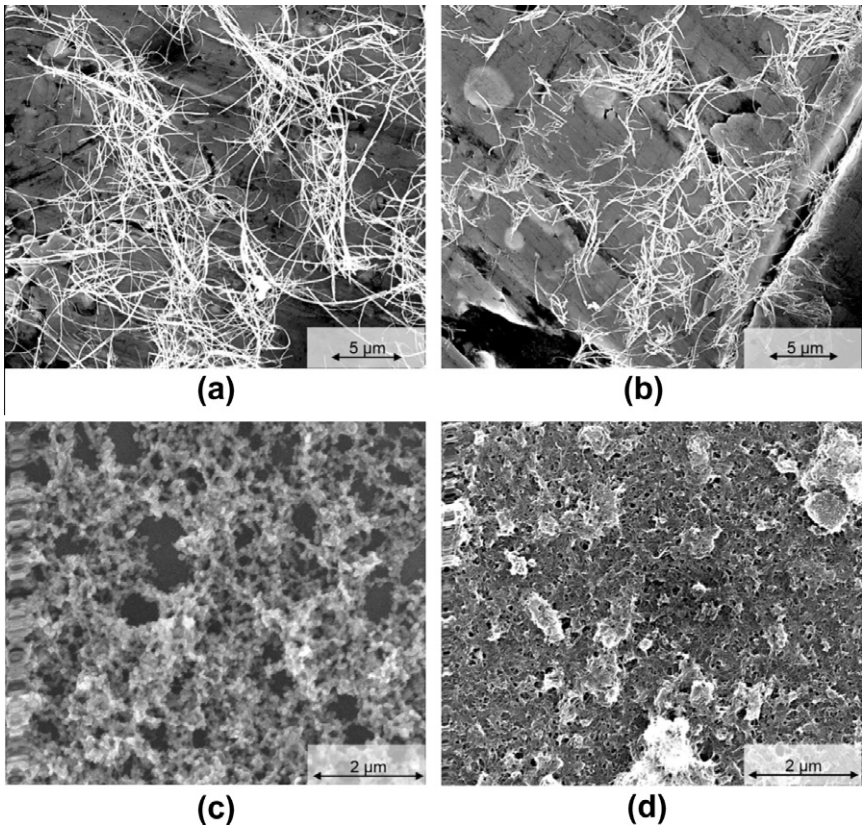

Fig. 8. SEM images of the dispersion films of N-CNTs (a and b) and mixed CNTs (c and d) after sonication for 30 min (a and c) and 150 min (b and d); CNT-to-SDS weight ratio 1:1.

cement. This can be explained by the high porosity of the samples containing SDS (Fig. 10a), caused by the formation of foam. In contrast, Brij 35 had significant influence neither on strength nor on porosity. No distinct increases in compressive and tensile strengths were observed after modifying the cement paste with CNTs in a concentration of 0.05% by weight of cement in comparison with

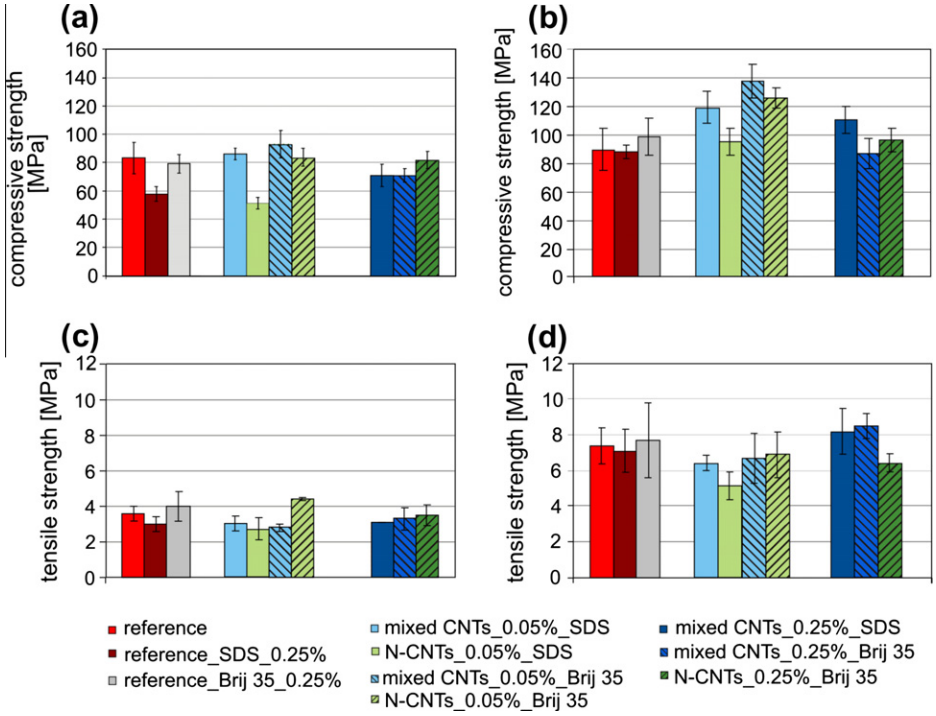

Fig. 9. Compressive and tensile strength of hardened cement paste at an age of 28 days subjected to quasi-static (a and c) and dynamic (b and d) loading. The indicators represent standard deviations.

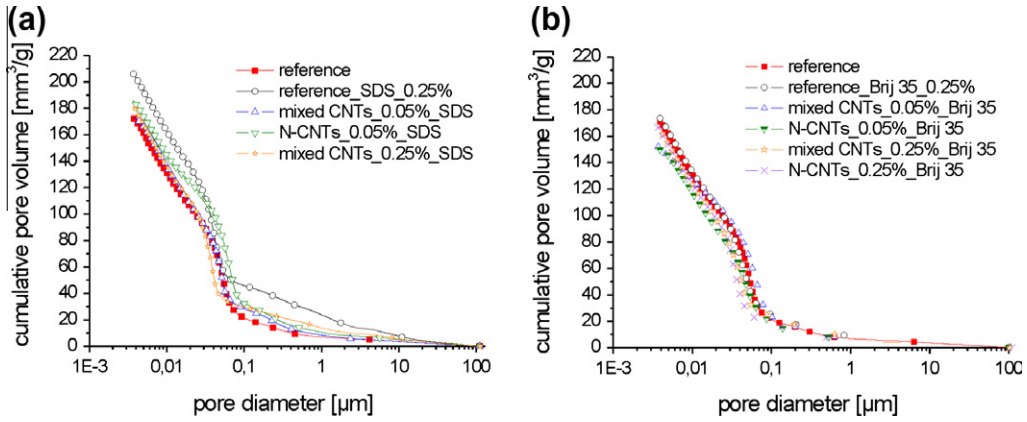

Fig. 10. Cumulative pore volume of hardened cement paste at an age of 28 days determined by mercury intrusion porosimetry.

the reference sample. These results are in disagreement with the findings of some previous investigations, e.g. [10,11]. The reduced negative effect of SDS in combination with mixed CNTs, which may be explained by its adsorption on the CNT surface, is worthy of note. Due to the adsorption the concentration of free surfactant molecules in the water is reduced; thus, the tendency towards micelle or foam formation is likewise reduced. In contrast, the selective adsorption of SDS on N-CNT surfaces gives rise to a high concentration of surfactant in water, which leads to foam formation and, consequently, high porosity of the cement paste. An increase in the CNT content of up to 0.25% by cement weight demonstrates no positive influence on strength, although the porosity is only slightly altered; cf. Fig. 10.

At a high strain rate, the negative influence of SDS on compressive strength is reduced; cf. Fig. 9b. The pore volume of the hardened cement paste was filled with water absorbed in the storage of samples in water prior to testing. According to [37,38], the water in pores contributes considerably to an increase in compressive strength in the case of dynamic loading. The capillary pressure increases with increasing strain rate, and a uniform stress state develops volume in the hardened cement. In this way the incompressible free water contributes to the load-bearing capacity of the hardened cement paste. The strength-increasing effect of CNTs in low concentrations is particularly noteworthy. The compressive strength of the hardened cement paste containing Brij 35 was improved by 40% using the mixed CNTs and by 30% using the N-CNTs. The increase in strength in the samples where SDS was used totalled 35% and 12% for the mixed and nitrogen-doped CNTs, respectively. An increase in CNT content to 0.25% by weight of cement had no clear positive influence. It should be noted that due to the small specimen sizes the standard deviation in the results was relatively high. However, since at least ten specimens were tested for each parameter combination, the average values can be considered trustworthy.

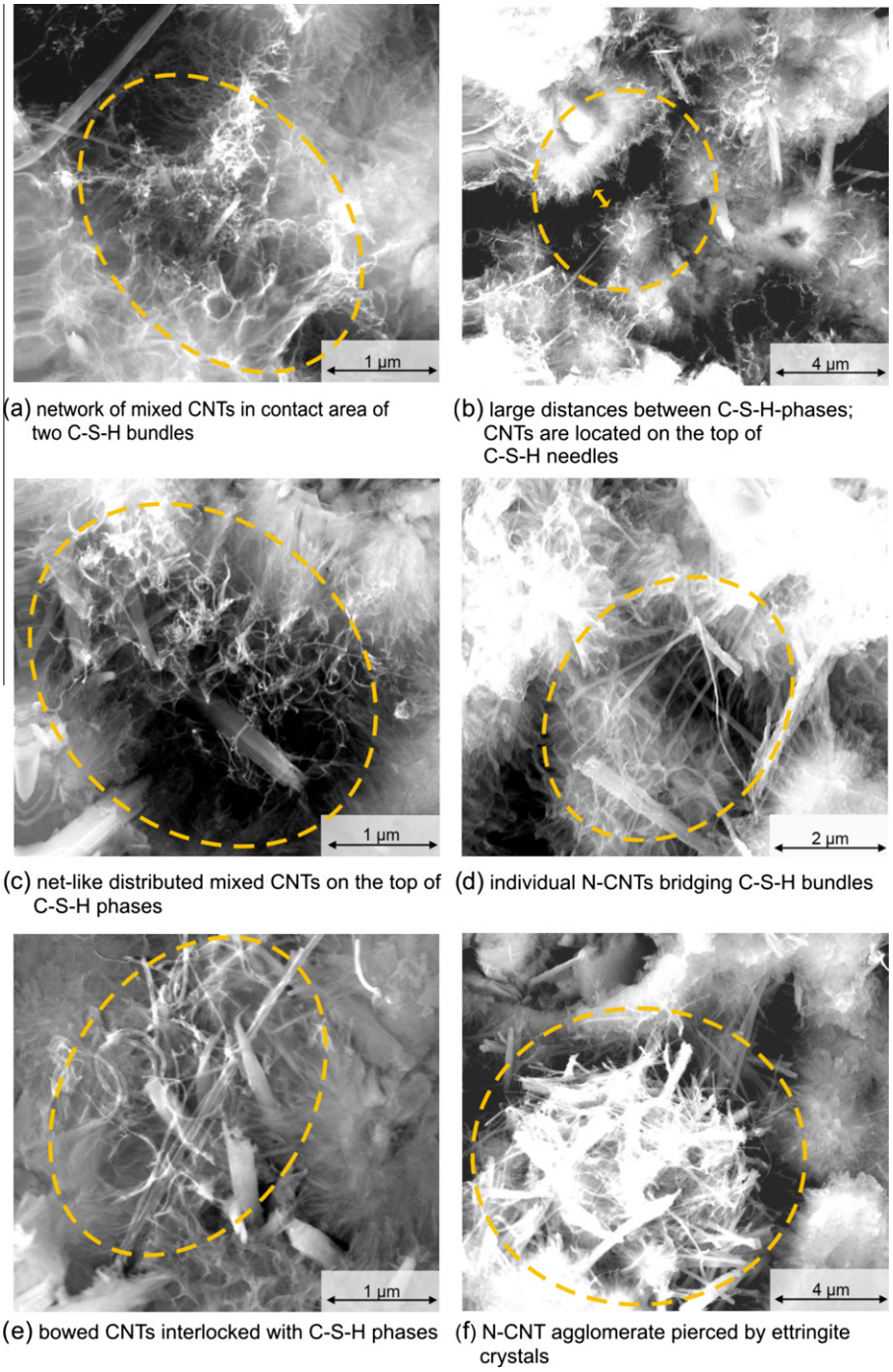

Fig. 11. ESEM images of hardened cement paste at an age of 3 days: cement paste modified with 0.05% of mixed CNTs (a–c); modification with 0.05% of N-CNTs (d–f); Brij 35 was used as surfactant.

Fig. 9d shows the results of tensile-strength testing at a high strain rate. The values of dynamic tensile strength were found to be generally higher that those measured under quasi-static loading, but no clear effect of the individual CNT types and contents on the dynamic tensile strength could be observed. However, the dynamic stress increase factor (the quotient of the dynamic and quasi-static tensile strengths), increased for the cement paste with mixed CNTs, especially at a high concentration of 0.25%.

The characterisation of the hydrated cement paste structure was performed with an environment scanning electron microscope (ESEM) using a Helix detector. Due to the dense arrangement of the hydration products at an age of 28 days, the CNTs in the cement matrix could barely be distinguished. Accordingly, fractured surfaces of the hardened cement paste were investigated at an age of three days in order to observe the distribution and condition of CNTs. Fig. 11a shows mixed CNTs in a net-like arrangement located at the tips of cement hydration products (C–S–H phases). The network formed of mixed CNTs is only capable of bridging distances smaller than 1 µm between C–S–H phases. Larger hollow spaces between hydration products could not be bridged; cf. Fig. 11b and c. In the case of the samples with N-CNTs, no net-like arrangement was observed. Only isolated CNTs which bound together individual C–S–H clusters were found; cf. Fig. 11d. As a result of ruptures during dispersion and bending, the majority of the

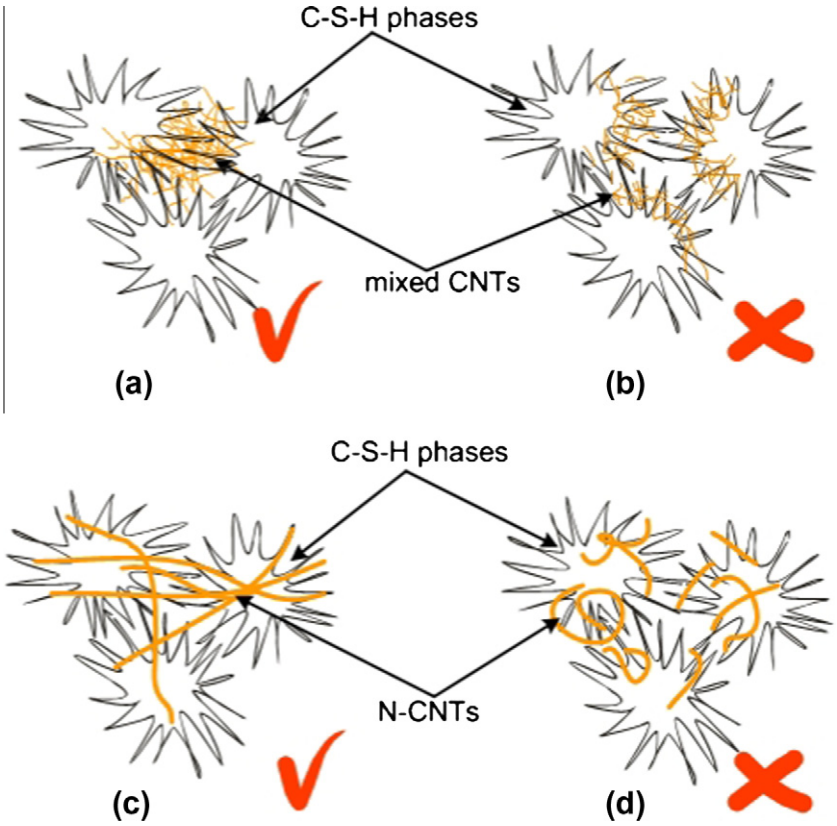

Fig. 12. Schematic representation of the arrangement of CNTs in a cement matrix: advantageous (a and c) and disadvantageous (b and d) distribution of the mixed CNTs and N-CNTs, respectively.

CNTs were not long enough to bridge the large distances between C–S–H phases. Furthermore, the bowing of the CNTs contributed to the reduction of their effective length (Fig. 11e).

Based on the results of the mechanical tests and microscopic investigations of the hydrated cement paste, it can be assumed that the network formation of mixed CNTs can bridge small distances of approximately 1 μm between the C–S–H phases and thus strengthen the interlocking of needle-like C–S–H crystals; cf. Fig. 12a. When hardened cement paste is slowly loaded, a crack originates in the place of the lowest resistance, which is generally located in the contact zone between the C–S–H phases and develops over a mainly tortuous path of low resistance. At a higher strain rate, however, due to limited time, the crack has to go straight through the CNT-reinforced area of the interlocking C–S–H formations. As a result of the greater strength and elasticity modules of the CNTs there, it meets greater resistance. Accordingly, higher stress is needed for the development of the crack and fracture of material. The concentration of the CNTs as well as the size of voids between the neighbouring C–S–H clusters seem to play a significant role here; cf. Fig. 12a and b. Furthermore, the storage of CNTs between the C–S–H needles can also impede interlocking. Due to the shortening of N-CNTs during dispersion, two neighbouring C–S–H clusters could be bound together (cf. Fig. 12c) in few cases only, such that no increase in tensile strength was observable. Mainly short and bowed CNTs were found, which exercised no strengthening effect (Fig. 12d).

The schematic presentations in Fig. 12 should provide a first general idea of the working mechanisms of the investigated types of CNTs in hardened cement paste. Here it should be underlined again that the foregoing discussions are based on the investigation of cement paste samples at an age of 3 days. Due to the densification of the matrix during the continuing cement hydration, the degree and possibly even the mode of interaction between the cement matrix and CNTs at greater ages might change significantly. There is a need for further research in this field. Accordingly, not all findings with respect to mechanical properties as presented in this report can be discussed in detail and explained at this stage. Furthermore, additional efforts should be focused on improving the dispersion methodology. In order to ensure the initial length of the N-CNTs, either another dispersion method or ultrasonication at lower amplitudes must be explored.

4. Conclusions

To make use of the positive effects of CNTs on the mechanical properties of cement-based composites, an appropriate dispersion of CNTs is mandatory. Preparation of CNT-dispersions is a challenging task since CNTs agglomerate both strongly and readily. In this paper, the dispersibility in water of two different types of CNTs was investigated by sonication in the presence of surfactants. The most advantageous dispersions could be produced with a CNT-to-surfactant ratio of 1:1–1:1.5 and a sonication time of 120 min. For the nitrogen-doped CNTs a combination with the surfactant Brij 35 led to a particularly intensive deagglomeration, which can be attributed to the good affinity between the Brij 35 molecules and the surfaces of the N-CNTs and consequently a homogeneous coating of CNT-surfaces. However, the N-CNTs tended to rupture with increasing sonication time. In contrast, no failure of the mixed CNTs could be observed, likely due to the formation of a fine CNT-network during dispersion, which prevented destruction by strong cavitation. For the mixed CNTs, no clear difference in dispersibility was observed between the use of SDS and the use of Brij 35 as surfactants.

For hardened cement paste modified with the CNTs, a pronounced increase in its compressive strength was determined under high strain rate loading. However, no significant improvement in strength was observed for quasi-static loading. The use of SDS as a surfactant had a negative effect on strength due to foam formation during the mixing of the cement paste. Microscopic examination of the hydrated cement paste structure showed the CNTs, depending on their type, to be arranged either as a discontinuous network or as individual fibres. Due to their insufficient length caused by fracturing during sonication and by misalignment attributable to twisting and curling, CNTs were mostly unable to satisfactorily bind neighbouring C–S–H clusters and to bridge the voids between them. This might explain the lack of improvement in the tensile strength of the cement matrix. Further research should be focused on achieving particular configurations of CNTs in the hardened cement paste, which would assure considerable improvements in its mechanical performance.

References

[1] Yu MF, Lourie O, Dyer M, Moloni K, Kelly T. Strength and breaking mechanism of multi-walled carbon nanotubes under tensile load. Science 2000;287:637–40.

[2] Salvetat JP, Borard JM, Thomson NH, Kulik AJ, Farro L, Bennit W, et al. Mechanical properties of carbon nanotubes. J Appl Phys A 1999;69:255–60.

[3] Li C, Chou TW. Elastic moduli of multi-walled carbon nanotubes and the effect of van der Waals forces. Compos Sci Technol 2003;63:1517–24.

[4] Khandoker N, Hawkins SC, Ibrahim R, Huynh CP, Deng F. Tensile strength of spinnable multiwall carbon nanotubes. Proc Engineer 2011;10:2572–8.

[5] Thostanson ET, Ren Z, Chou TW. Advances in the science and technology of carbon nanotubes and their composites: a review. Compos Sci Technol 2001;61:1899–912.

[6] Bonard JM, Maier F, Stöckli T, Châtelain A, de Heer WA, Salvetat JP, et al. Field emission properties of multiwalled carbon nanotubes. Ultramicroscopy 1998;73:7–15.

[7] Paiva MC, Zhou B, Fernando KAS, Lin Y, Kennedy JM, Sun YP. Mechanical and morphological characterization of polymer–carbon nanocomposites from functionalized carbon nanotubes. Carbon 2004;42:2849–54.

[8] Yang BY, Shi JH, Pramoda KP, Goh SH. Enhancement of the mechanical properties of polypropylene using polypropylene-grafted multiwalled carbon nanotubes. Compos Sci Technol 2008;68:2490–7.

[9] Moniruzzaman M, Winey KI. Polymer nanocopmosites containing carbon nanotubes. Macromolecules 2006;39:5194–205.

[10] Konsta-Gdoutos MS, Metaxa ZS, Shah SP. Multi-scale mechanical and fracture characteristics and early-age strain capacity of high performance carbon nanotube/cement nanocomposites. Cem Concr Compos 2010;32:110–5.

[11] Li GY, Wang PM, Zhao X. Mechanical behavior and microstructure of cement composites incorporating surface-treated multi-walled carbon nanotubes. Carbon 2005;43:1239–45.

[12] Makar J, Margeson J, Luh J. Carbon nanotube/cement composites – early results and potential applications. In: Proceedings of the 3rd international conference on construction materials: performance, innovations and structural implications, Vancouver, BC, Canada, August 22–24, 2005.

[13] Musso S, Tulliani J-M, Ferro G, Taglaferro A. Influence of carbon nanotubes structure on the mechanical behavior of cement composites. Compos Sci Technol 2009;69:1985–90.

[14] Konsta-Gdoutos MS, Metaxa ZS, Shah SP. Highly dispersed carbon nanotube rein forced cement based materials. Cem Concr Res 2010;40:1052–9.

[15] Luo J, Duan Z, Li H. The influence of surfactants on the processing of multi-walled carbon nanotubes in reinforced cement matrix composites. Phys Status Solidi A 2009;206(12):2783–90.

[16] Xie X-L, Mai Y-W, Zhou X-P. Dispersion and alignment of carbon nanotubes in polymer matrix: a review. Mat Sci Eng 2005;R49(4):89–112.

[17] Sàes de Ibarra Y, Gaitero JJ, Erkizia E, Campillo I. Atomic force microscopy and nanoindentation of cement pastes with nanotube dispersions. Phys Status Solid A 2006;203(6):1076–81.

[18] Krause B, Ritschel M, Täschner Ch, Oswald S, Gruner W, Leonhard A, et al. Comparison of nanotubes produced by fixed bed and aerosol-CVD methods and their electrical percolation behaviour in melt mixed polyamide 6.6. composites. Compos Sci Technol 2010;70:151–60.

[19] Jiang L, Gao L, Sun J. Production of aqueous colloidal dispersion of carbon nanotubes. Colloid Interface Sci 2003;260:89–94.

[20] Miltner HE, Grossiord N, Lu K, Loos J, Koning CE, van Mele B. Isotactic polypropylene/carbon nanotube composites prepared by latex technology. thermal analysis of carbon nanotube-induced nucleation. Macromolecules 2008;41(15):5753–62.

[21] Chapell MA, George AJ, Dontsova KM, Porter BE, Price CL, Zhou P, et al. Surfactive stabilisation of multi-walled carbon nanotubes dispersion with dissolved humic substances. Environ Poll 2009;157:1081–7.

[22] Rausch J, Zhuang RC, Mäder E. Surfactant assisted dispersion of functionalized multi-walled carbon nanotubes in aqueous media. Composites 2010:1038–46.

[23] Grossiord N, Regev O, Loos J, Meuldijk J, Koning CE. Time-dependent study of the exfoliation process of carbon nanotubes in aqueous dispersion by using UV–vis spectroscopy. Anal Chem 2005;77:5135–9.

[24] Rastogi R, Kaushal R, Tripathi SK, Sharma AL, Kaur I, Bharadwaj LM. Comparative study of carbon nanotube dispersion using surfactants. Colloids Interface Sci 2008;328:421–8.

[25] Adler YP. Introduction to experimental design. Moscow; 1969 [in Russia].

[26] Synoradzki L, Jańczewski D, Włostowski M. Optimisation of ethyl(2-phthalimidoethoxy)acetate synthesis with the aid of DOE. Organ Process Res Dev 2005;9:18–22.

[27] Mubarak NM, Yusof F, Alkhatib MF. The production of carbon nanotubes using two-stage chemical vapor deposition and their potential use in protein purification. Chem Eng J 2011;168:461–9.

[28] Dörfler HD. Grenzflächen- und Kolloidchemie. Weinheim: VCH; 1994.

[29] Little EL, Foley JP. Optimization of the resolution of PTH-amino acids through control of surfactant concentration in micellar electrokinetic capillary chromatography: SDS vs. Brij 35/SDS micellar systems. Microcol Separ 1992;4:145–54.

[30] Hait SH, Moulik SP. Determination of critical concentration (CMC) of nonionic surfactants by donor-acceptor interaction with iodine and correlation of CMC with hydrophile-lipophile balance and other parameters of the surfactants. Surfact Deter 2001;4(3):303–8.

[31] Chappell MA, Laird DA, Thompson ML, Evangelou VP. Co-sorption of atrazine and lauryl polyoxyethylene oxide nonionic surfactant on smectite. Agric Food Chem 2005;53:10127–33.

[32] Tao XY, Zhang XB, Sun FY, Cheng JP, Liu F, Luo ZQ. Large-scale CVD synthesis of nitrogen-doped multi-walled carbon nanotubes with controllable nitrogen content on a $Co_xMg_{1-x}MoO_4$ catalyst. Diamond Relat Mater 2007;16:425–30.

[33] Maldonado S, Morin S, Keith JS. Structure, composition, and chemical reactivity of carbon nanotubes by selective nitrogen doping. Carbon 2006;44:1429–37.

[34] Fu SY, Chen ZK, Hong S, Han CC. The reduction of carbon nanotube (CNT) length duting the manufacture of CNT/polymer composites and a method to simultaneously determine the resulting CNT and interfacial strengths. Carbon 2009;47:3192–200.

[35] Chowdhury DF, Cui ZF. Carbon nanotube length reduction techniques, and characterisation of oxidation state using quasi-elastic light scattering. Carbon 2011;49:862–8.

[36] Meier M, Andrews R, Jacques D, Cassity KB, Qian D. Tearing open nitrogen-doped multiwalled carbon nanotubes. J Mater Chem 2008;18:4143–5.

[37] Rossi P. Influence of cracking in the presence of free water on the mechanical behaviour of concrete. Mag Concr Res 1991;154:53–7.

[38] Larcher M. Numerische Simulation des Betonverhaltens unter Stoßwellen mit Hilfe des elementfreien Galerkin-Verfahrens. Dissertation. Karlsruhe: Universität Karlsruhe; 2007.